Elliptical Contourlet Transform and Its Application to Image Representation

Bushra.A.Taha

Department of Mathematics, College of Science, Basrah University

Basrah,Iraq.

Abstract

This paper introduces a new form of contourlet transform called "elliptical contourlet transform" is proposed based on elliptically-support and directionally-decomposed filter bank structures. The comparison of such elliptical contourlet transform with the classical contourlet transform proves its superiority in both subjective and objective measurement.

Keywords: filter banks, directional filter banks(**DFBs**), contourlet transform ,elliptical filter banks**(EFBs)**.

1.Introduction

(Do M. N. , Vetterli M. 2003,2005) and (Po D. Y. D. , Do M. N.2004) developed the contourlet transform based on an efficient two-dimensional multiscale and directional filter bank that can deal effectively with images having smooth contours. Contourlets not only possess the main features of wavelets(Mallat M.1998)namely, multiscale and time-frequency localization), but also offer a high degree of directional and anisotropy. The main difference between contourlets and other multiscale directional systems is that the contourlet transform allows for different and flexible number of directions at each scale, while achieving nearly critical sampling. In addition, the contourlet transform uses iterated filter banks ,which makes it computationally efficient; specifically, it requires $O(N)$ bytes of memory and NxN filtering operations for an N -pixel image.

The contourlet transform is one of the new geometrical image transforms, which can efficiently represent images containing contours and textures. In the contourlet transform, a Laplacian pyramid (LP)(Burt P. J.,Adelson H.1983, Do M. N., Vetterli M.2003)is employed for the first stage, while directional filter banks (DFB)(Abdul-Jabbar J. M 1997)are used in the angular decomposition stage(the

number of band directional filter banks is 2^n , $n = 1,2,3,...$).With this insight, a double filter bank structure is used (see Figure(1)) to obtain sparse expansions for typical images having smooth contours. In this double filter bank, the Laplacian pyramid is first used to capture the point discontinuities, and then followed by a directional filter bank to link point discontinuities into linear structures. The overall result is an image expansion using basic elements like contour segments, and thus are named contourlets.

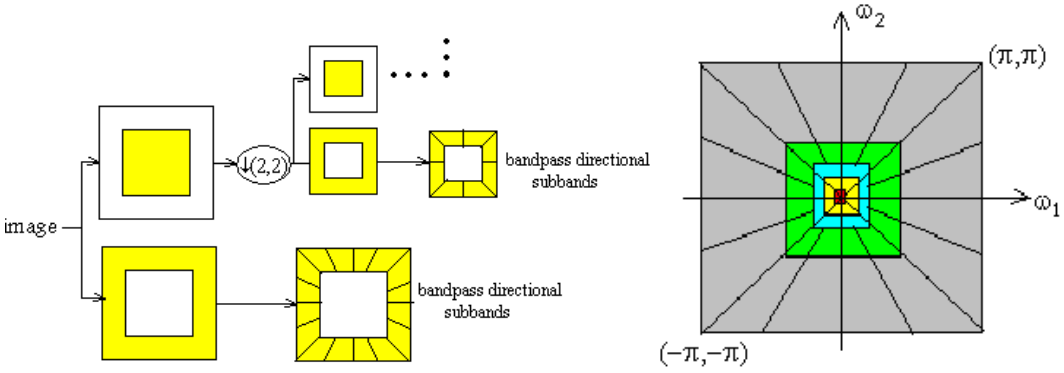

(a) *(b)*

Figure(1) (a) The contourlet filter bank: first, a multiscale decomposition into octave bands by the Laplacian pyramid is computed, and then a directional filter bank is applied to each bandpass channel.(b) A typical contourlet frequency partition scheme.

2. Laplacian Pyramid

One way of achieving a multiscale decomposition is to use a Laplacian pyramid (LP) as introduced by Burt and Adelson,1983. The LP decomposition at each step generates a sampled lowpass version of the original and the difference between the original and the prediction, resulting in a band pass image (see Figure(2a)). We show that the LP with orthogonal filters (that is , $h[n] = g[-n]$ and $g[n]$ is orthogonal to its translates with respect to the subsampling lattice)is a tight frame with frame bounds equal to one (Do M. N.,Vetterli M.2005). In this case, we suggest the use of the optimal linear reconstruction using the dual frame operator, which is symmetrical with the forward transform(see Figure(2b)).Note that, this new reconstruction is different from the usual reconstruction and is crucial for our contourlet expansion .

3. Design of Analysis and Synthesis Filters

Matrix/vector notations have been used for the description of multirate operations in two dimensions. These descriptions enable relationships for multirate operations to be expressed in a form which resembles that of their one-dimensional counterparts. To lay the ground for discussion, some notational conventions and definitions used in this research are mentioned first. A filter bank consists of a decomposition stage and a recombination stage . In the decomposition

stage a signal x is convolved with a low–pass filter h and high-pass filter g, followed by sub-sampling the results by a factor of two, yielding(Abdul-Jabbar J. M,1997,Mallat M.1998, Bamberger R. H.,Smith M.1992).

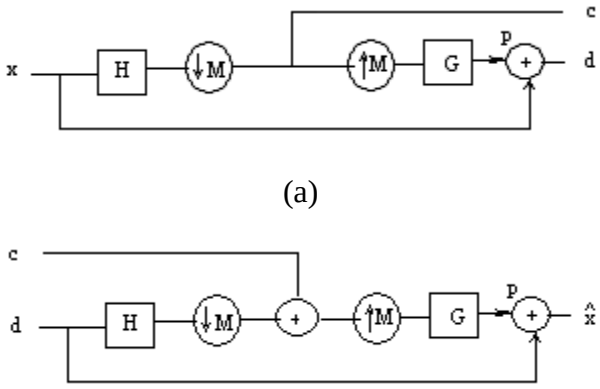

Figure (2): Laplacian pyramid scheme.(a) Analysis: the outputs are a coarse approximation c and a difference d between the original signal and the prediction. The process can be iterated by decomposing the coarse version repeatedly. (b) The proposed reconstruction scheme for the Laplacian pyramid.

$$a = x * h[2n] \quad and \quad d = x * g[2n] \tag{1}$$

The reconstruction stage convolves the up-sampled (zero-interleaved) versions of a and d with the reconstruction filter $\tilde{h}$ and $\tilde{g}$ (see Figure (3)):

$$\hat{x} = \breve{a} * \tilde{h}[n] + \breve{d} * \tilde{g}[n]. \tag{2}$$

The most general relation between $\hat{x}(z)$ and $x(z)$ is given by

$$\hat{x}(z) = \frac{1}{2}[\tilde{h}(z)h(z) + \tilde{g}(z)g(z)]x(z) + \frac{1}{2}[\tilde{h}(z)h(-z) + \tilde{g}(z)g(-z)]x(-z) \tag{3}$$

second term in (3) represents to the effect of aliasing. However, for aliasing case,

$$h(-z)\tilde{h}(z) + g(-z)\tilde{g}(z) = 0 \tag{4}$$

and

$$\frac{1}{2}\left[h(z)\tilde{h}(z) + g(z)\tilde{g}(z)\right] = \frac{\hat{x}(z)}{x(z)} = T(z) \tag{5}$$

where $z = e^{i\omega}$ (i=$\sqrt{-1}$), and $T(z)$ is the distortion function. The solution of ordinary quadrature mirror filter (QMF) is obtained by choosing the filters so as to satisfy

$$\left.\begin{aligned} g(z) &= h(-z) \\ \tilde{h}(z) &= g(-z) = h(z) \\ \tilde{g}(z) &= -h(-z) = -g(z) \end{aligned}\right\} \tag{6}$$

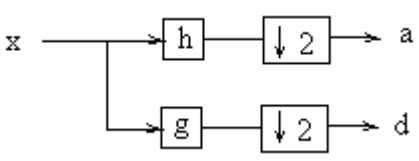

(a) analysis

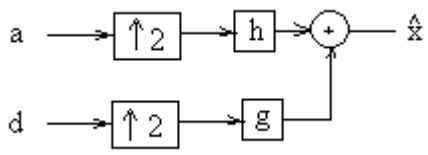

(b) synthesis

Figure (3): (a) The analysis step convolves x with filters h, g , followed by sub-sampling by a factor of 2 (retaining only the even entries). (b) The synthesis step takes as input an average, a , and detail, d .

We can write (5) as

$$\hat{x}(z) = \frac{1}{2}\left[h^2(z) - g^2(z)\right]x(z) \qquad (7)$$

or

$$\hat{x}(z) = \frac{1}{2}\left[h^2(z) - h^2(-z)\right]x(z)$$

On the unit circle, for all ω

$$\left|h^2(e^{i\omega}) - h^2(e^{i\omega+\pi})\right| = 1 \qquad (8)$$

then, the total system gain will be unity. Since condition (8) does not impose any phase characteristics. It is not enough to satisfy equation(5).

The problem has now been reduced to the design of the filter $h(e^{i\omega})$ which approximates the ideal low-pass condition, i.e., that (Abdul-Jabbar J. M.1997)

$$h(e^{i\omega}) = \begin{cases} 1 & 0 \le \omega \le \pi/2 \\ 0 & \pi/2 \le \omega \le \pi \end{cases} \qquad (9)$$

The conditions (8) and (9) can be simultaneously met. However, they can be closely approximated using some numerical techniques.

$$\left|h(e^{i\omega})\right|^2 + \left|g(e^{i\omega})\right|^2 = 1 \quad \text{,for all } \omega \qquad (10)$$

The condition (10) must be fulfilled if we want to express $h(z)$ and $g(z)$(as the sum and difference of all-pass sections. It is pointed there that the necessary and sufficient condition for a transfer function $h(z)$ or $g(z)$ to be realizable as the sum or difference of two all-pass functions, respectively, is that the characteristic functions

$$\frac{g(z)}{h(z)} \quad \text{or} \quad \frac{h(z)}{g(z)}$$

They were previously odd rational functions which then are transformed via the bilinear transformation. If the above condition is taken into account, we can write

$$h(z) = \frac{1}{2}\left[\, a_0(z) + a_1(z) \,\right] \qquad (11.a)$$

and

$$g(z) = \frac{1}{2}\left[\, a_0(z) - a_1(z) \,\right], \qquad (11.b)$$

where $a_0(z)$ and $a_1(z)$ are stable (Abdul-Jabbar J. M.1997)all-pass functions which can be represented as

$$a_i(z) = \frac{z^{-n_i} D_i(z^{-1})}{D_i(z)} \qquad for \quad i = 0,1 \qquad (12)$$

Here $D_i(z)$ is Hurwitz polynomial of degree n_i .

The structure in Figure (3,a-b) represents the lattice all-pass equivalence of the analysis and synthesis bank is shown in Figure (4, a- b), in

which the 2-band analysis bank is represented in the form of the sum and difference of the two all-pass filters.

The two square spectrum filters $G_0(z_1,z_2)$ and $G_1(z_1,z_2)$ can then be formed where

$$G_0(z_1,z_2)=h(z_1)\,h(z_2) \qquad (13.a)$$

And

$$G_1(z_1,z_2)=g(z_1)\,g(z_2) \qquad (13.b)$$

Hence, the checkerboard filters can be formed as(Do M. N.,Vetterli M.,2003,2005)

$$C_0(z_1,z_2)=G_0(z_1,z_2)+G_0(-z_1,-z_2) \qquad (14.a)$$

and

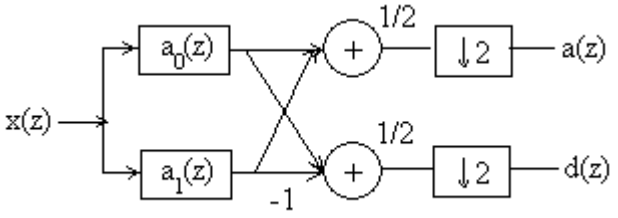

(a)

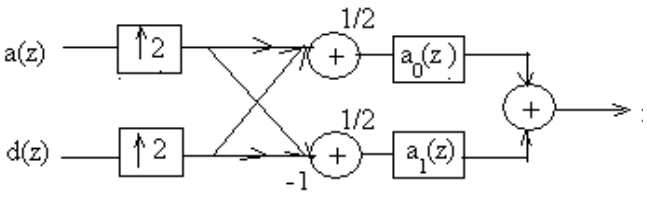

(b)

Figure (4): (a)The analysis bank. (b) The synthesis bank.

$$C_1(z_1,z_2)=G_1(z_1,z_2)+G_1(-z_1,-z_2) \qquad (14.b)$$

This in turn leads to the following expressions:

$$C_0(z_1,z_2)=\frac{1}{2}\left[A_0(z_1,z_2)+A_1(z_1,z_2)\right] \qquad (15.a)$$

$$C_1(z_1,z_2)=\frac{1}{2}\left[A_0(z_1,z_2)-A_1(z_1,z_2)\right] \qquad (15.b)$$

where the 2-D all-pass functions $A_0(z_1,z_2)$ and $A_1(z_1,z_2)$ are defined as

$$A_0(z_1,z_2)=a_0(z_1)\,a_0(z_2) \qquad (16.a)$$

and

$$A_1(z_1,z_2)=a_1(z_1)\,a_1(z_2) \qquad (16.b)$$

where

$$a_0(z)=\frac{z^{-1}\,D_0(z^{-1})}{D_0(z)}=\prod_{l=0,\,even}^{\frac{N-1}{2}}\frac{z^{-1}-\delta_l}{1-\delta_l\,z^{-1}} \qquad (16.c)$$

$$=\frac{z^{-1}-\delta_0}{1-\delta_0\,z^{-1}}\prod_{l=2,\,even}^{\frac{N-1}{2}}\frac{z^{-2}-2\,u_l\,z^{-1}+r_l^2}{1-2\,u_l\,z^{-1}+r_l^2\,z^{-2}}$$

$$a_1(z)=\frac{z^{-1}\,D_1(z^{-1})}{D_1(z)}=\prod_{l=1,\,odd}^{\frac{N-3}{2}}\frac{z^{-1}-\delta_l}{1-\delta_l\,z^{-1}} \qquad (16.d)$$

$$=\prod_{l=1,\,odd}^{\frac{N-1}{2}}\frac{z^{-2}-2\,u_l\,z^{-1}+r_l^2}{1-2\,u_l\,z^{-1}+r_l^2\,z^{-2}}$$

Where $\delta_0,\delta_1,...,\delta_{(N-1)/2}$ are the N poles of the transfer function $h(z)$ of the reference filters. It can be seen that, δ_0 is real, while the others

$\delta_i=u_i+j\,v_i \quad for\ i=1,2,...,\frac{(N-1)}{2}$, and also $r_i^2=u_i^2+v_i^2$.

The same efficient realization of (16.a) and (16.b)can also be used to implement the 2-D synthesis filter banks.

4. 2-band directional-decomposed split scheme

This type of split scheme is an n-shifted version of the diamond type in either ω_1 or ω_2 axis. It also leads to a non-separable filter banks, which can be directly transformed to $A_0(z_1', z_2')$ and $A_1(z_1', z_2')$, where

$$A_i(z_1', z_2') = A_i(z_1, z_2) \quad for \ i = 0,1 \qquad (17)$$

where

$$z_1 = \sqrt{-z_1' \ z_2'} \quad , \quad z_2 = \sqrt{-z_1' (z_2')^{-1}}$$

Now, we can design and efficiently implement a 2-band directionally-decomposed filter bank,which has a zero-phase response. If the specifications of reference filter-1 is used, the corresponding tow directional (2-D) all-pass functions (non separable) $A_0(z_1', z_2')$ and $A_1(z_1', z_2')$ can be formed as

$$A_0(z_1', z_2') = a_0(\sqrt{-z_1 \ z_2}) \ a_0(\sqrt{-z_1 \ z_2^{-1}})$$

and

$$A_1(z_1', z_2') = a_1(\sqrt{-z_1 \ z_2}) \ a_1(\sqrt{-z_1 \ z_2^{-1}})$$

The directionally-decomposed filter bank transfer functions $DA_0(z_1, z_2)$ and

$DA_1(z_1, z_2)$ can be written in matrix form as

$$\begin{bmatrix} DA_0(z_1, z_2) \\ DA_1(z_1, z_2) \end{bmatrix} = \frac{1}{2} \begin{bmatrix} 1 & 1 \\ 1 & -1 \end{bmatrix} \begin{bmatrix} A_0(z_1, z_2) \\ A_1(z_1, z_2) \end{bmatrix}$$

The resulting 2-band directionally-decomposed filter bank can be implemented as in Figure(3.a-b),but with $a_0(z)$ and $a_1(z)$ being replaced by $A_0(z_1', z_2')$ and $A_1(z_1', z_2')$ as given in (17), respectively. The resulting responses $DA_0(\omega_1, \omega_2)$ and $DA_1(\omega_1, \omega_2)$ are shown in Figure (5,a -b), respectively.

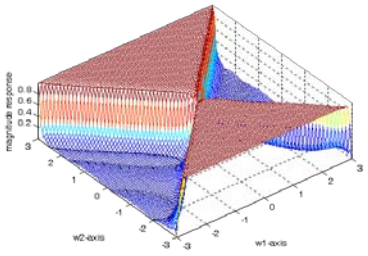

(a)

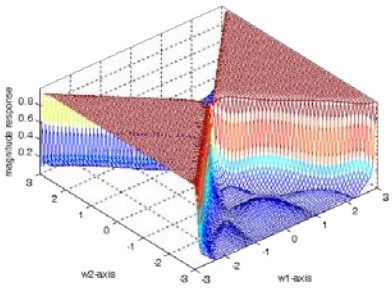

(b)

Figure (5): 2-band directionally-decomposed filter bank responses

(a) $DA_0(\omega_1, \omega_2)$ (b) $DA_1(\omega_1, \omega_2)$

5. 4-band directional-decomposed split scheme

This spilt scheme is approached here by using two-stage tree structure. The first stage is a 2-band fan filter. This is cascaded with a second stages which has the 2-band quadrant filter bank in a tree structure manner. The two stage are implemented in the commonly mentioned zero-phase IIR(Abdul-Jabbar J.

M.1997) lattice all-pass structure. The analysis filter bank is shown in Figure(5), in which $A_0(z_1', z_2')$ and $A_1(z_1', z_2')$ are the same as those given in (17) . The other all-pass functions $B_0(z_1, z_2)$ and $B_1(z_1, z_2)$ are the same as those given by $A_i(z_1', z_2')$, *for* $i = 0,1$, where

$$A_i(z_1', z_2') = A_i(z_1, z_2), \quad z_1 = j\, z_1', z_2 = j\, z_2'$$

The two stages can be interchanged, but this will result in a more non-separable sub-systems. This is due to the fact that putting the quadrant filter bank as a second stage in the tree structure means that it will be used twice and since it is of the separable type, we guarantee the use of, as mush as possible, separable implementation. We can design a 4-band directionally-decomposed filter bank and implemented in an efficient manner by using the specifications given in reference filter (1), (Abdul-Jabbar J. M.,997) then the all-pass functions required in implementation of Figure(5), are given by

$$A_i(z_1', z_2') = a_i(\sqrt{-z_1\, z_2})\; a_i(\sqrt{-z_1\, z_2^{-1}}), \quad (18)$$

and

$$B_i(z_1', z_2') = a_i(j\, z_1)\; a_i(j\, z_2) \qquad for\ i = 0,1.$$

The 4-band directionally-decomposed filter bank transfer functions can be written as

$$DA_i'(z_1, z_2) = \frac{1}{4}\left[A_0(z_1, z_2) + A_1(z_1, z_2)\right]\left[B_0(z_1, z_2) \mp B_1(z_1, z_2)\right] \quad , \quad for\ i = 0,1. \qquad (a)$$

and

$$DA_i'(z_1, z_2) = \frac{1}{4}\left[A_0(z_1, z_2) - A_1(z_1, z_2)\right]\left[B_0(z_1, z_2) \mp B_1(z_1, z_2)\right] \quad , \quad for\ i = 2,3.$$

The resulting magnitude responses $DA_i'(\omega_1, \omega_2)$, *for* $i = 0,1,2,3.$ are shown in Figure(6,a- d), respectively. It should be pointed here that the synthesis bank for this type of filter banks is an identical reversal of the analysis bank, with one time

Similarly, 8-band directionally-decomposed filter bank can be designed by using the analysis in section 4-band . The corresponding 8-band directionally-decomposed filter bank transfer function can be written as

$$DA_i''(z_1, z_2) = \frac{1}{8}\left[A_0(z_1, z_2) + A_1(z_1, z_2)\right]\left[B_0(z_1, z_2) + B_1(z_1, z_2)\right]\left[C_0(z_1, z_2) \mp C_1(z_1, z_2)\right] \quad for\ i = 0,1$$

$$DA_i''(z_1, z_2) = \frac{1}{8}\left[A_0(z_1, z_2) + A_1(z_1, z_2)\right]\left[B_0(z_1, z_2) - B_1(z_1, z_2)\right]\left[C_0(z_1, z_2) \mp C_1(z_1, z_2)\right] \quad for\ i = 2,3$$

$$DA_i''(z_1, z_2) = \frac{1}{8}\left[A_0(z_1, z_2) - A_1(z_1, z_2)\right]\left[B_0(z_1, z_2) + B_1(z_1, z_2)\right]\left[C_0(z_1, z_2) \mp C_1(z_1, z_2)\right] \quad for\ i = 4,5$$

$$DA_i''(z_1, z_2) = \frac{1}{8}\left[A_0(z_1, z_2) - A_1(z_1, z_2)\right]\left[B_0(z_1, z_2) - B_1(z_1, z_2)\right]\left[C_0(z_1, z_2) \mp C_1(z_1, z_2)\right] \quad for\ i = 6,7$$

The resulting responses $DA_i''(\omega_1, \omega_2)$ *for* $i = 0,1,2,3,4,5,6,7$ are shown in Figure (7, a-h), respectively.

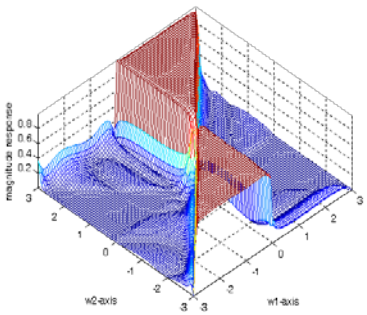

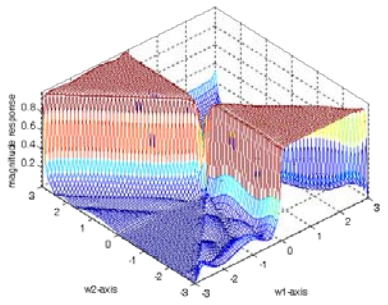

(b)

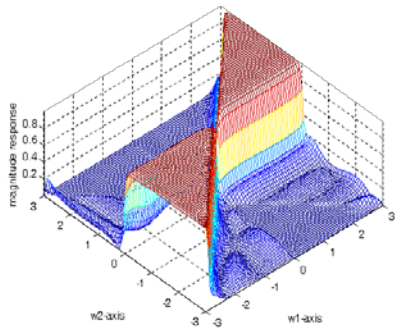

(c)

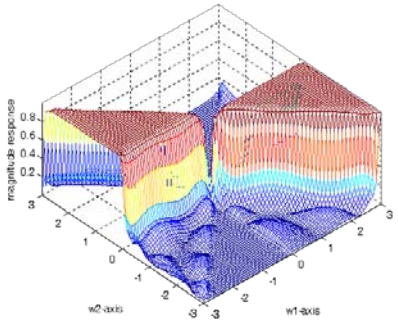

(d)

Figure (6): 4-band directionally-decomposed filter bank responses.

(a) $DA_0'(\omega_1,\omega_2)$ ***(b)*** $DA_1'(\omega_1,\omega_2)$

(c) $DA_2'(\omega_1,\omega_2)$ ***(d)*** $DA_3'(\omega_1,\omega_2)$

6. Elliptical contourlet split scheme

This is a new type of partitioning the 2-D signals. Elliptical split scheme or Elliptically – decomposed schemes permit the use of different sampling rates along the two spatial axes.

It should be noted ,here, that the elliptical decomposition scheme requires some nonlinear change of variables, such as

$$z_1' = f_1(z_1)\, f_2(z_2) \qquad (19a)$$

and

$$z_2' = f_1(z_1)\, f_2(z_2^{-1}) \qquad (19b)$$

where

$$f_i(z_i) = \frac{z_i + \alpha_i}{1 + \alpha_i\, z_i} \qquad for\ \ i = 1,2 \qquad (20)$$

with $\alpha_1 \neq \alpha_2$ for elliptical shape decomposition.

The choice of α_1 and α_2 values provides the appropriate bending for the supports to look like elliptical shapes. On the other hand, to insure stability the values of α_1 and α_2 are limited to:

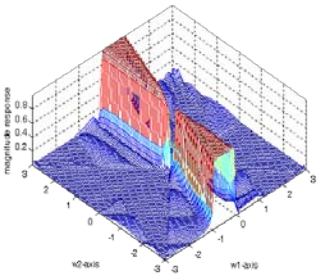

(a)

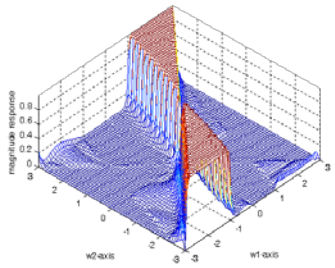

(b)

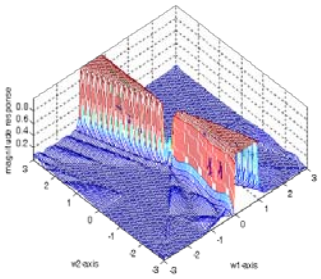

(c)

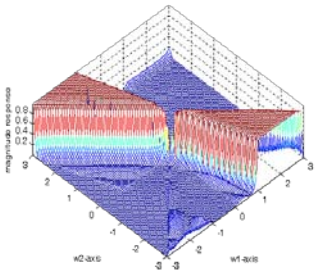

(d)

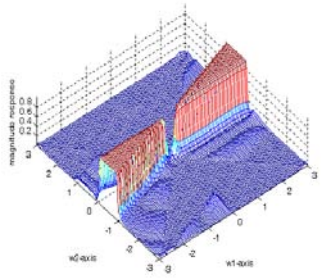

(e)

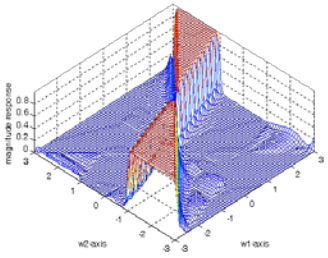

(f)

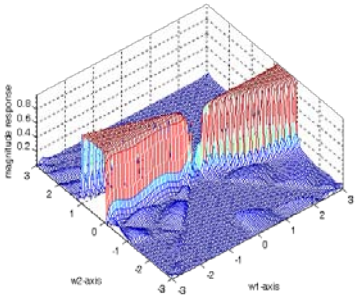

(g)

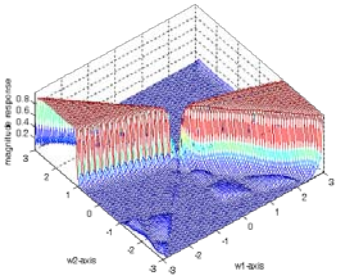

(h)

Figure (7): 8-band directionally-decomposed filter bank responses.

(a) $DA_0''(\omega_1,\omega_2)$ (b) $DA_1''(\omega_1,\omega_2)$ (c) $DA_2''(\omega_1,\omega_2)$ (d) $DA_3''(\omega_1,\omega_2)$

(e) $DA_4''(\omega_1,\omega_2)$ (f) $DA_5''(\omega_1,\omega_2)$ (g) $DA_6''(\omega_1,\omega_2)$ (h) $DA_7''(\omega_1,\omega_2)$

$$|\alpha_i| < 1 \qquad for\ i = 1,2. \tag{21}$$

It should be noted that the change of variables in equation(19)is a nonlinear transformation called the digital spectral transformation(DST) (Abdul-Jabbar J. M.1997) . Due to this non-linearity, these variations of variables cannot be readily incorporated in the sampling rate alteration filters. Therefore, such changes can be incorporated in the analysis/synthesis filters themselves, resulting in 2-D all-pass sections which are nonseparable, although they can be efficiently implemented as will be shown in the following discussion.

It is also required here to have a linear-phase(or even zero-phase) IIR filter bank implementation. Thus, the constraints (6-8) derived from Figure(2) are still applicable for elliptical decomposition. On the other hand, a simpler and efficient implementation than that of Figure (2) is also needed. From the power-complementary condition in equation(10), one can write for 1-D case,

$$\left| g(z) \right|^2 = 1 - \left| h(z) \right|^2 \qquad (22)$$

It can be easily shown that, in the passband,

$$\left| g(z) \right|^2 \cong \left| g(z) \right| \qquad (23)$$

Thus, one can write

$$\left| g(z) \right| = 1 - \left| h(z) \right|^2 \qquad (24)$$

Therefore, whatever is the phase response of $h(z)$, a zero-phase function $g(z)$ can be obtained when we choose $g(z) = 0$, i. e. ,

$$g(z) = \left| g(z) \right| \qquad (25)$$

From (24) and (25), we get

$$g(z) = 1 - \left| h(z) \right|^2 \qquad (26)$$

The elliptically-decomposed filter banks can be implemented with zero-phase by using the same one directional (1-D) structure ,but with $h(z)$ being transformed via the DST to $h(z_1, z_2)$ which is given by :

$$h(z_1, z_2) = h(z_1')\, h(z_2')\, h(f_1(z_1))\, h(f_2(z_2)) \qquad (27)$$

where z_1' and z_2' are as those given in (19,a-b) and $f_i(z_i)$ is as given in (20).

It has been previously proved that the application of this DST to a linear-phase 1-D filter leads to 2-D filters which preserve the linear-phase characteristics approximately. Thus, we can conclude that the application of this DST to the zero-phase 1-D filter banks, will lead to a 2-D elliptically directional filter banks(EDFB) (depending on values of α_1 and α_2), which preserve an approximate zero-phase overall response.

If the filter $h(z)$, is implemented in a lattice of cascaded all-pass sections, then some saving in computation can be gained. While lattice structure will provide the system with a reduced sensitivity to multiplier values finite word length.

Figure(8) show this type of 2-D magnitude responses. The cutoff curve,here, is given by the ellipse

$$\left[\frac{\omega_1}{\omega_{1c}} \right]^2 + \left[\frac{\omega_2}{\omega_{2c}} \right]^2 = 1$$

Where ω_{1c} *and* ω_{2c} are the two cutoff frequencies, one in each dimension. The passband is described by the region

$$\left\{ \omega_1, \omega_2 : \left[\left[\frac{\omega_1}{\omega_{1c}} \right]^2 + \left[\frac{\omega_2}{\omega_{2c}} \right]^2 \right] \le 1 \right\}$$

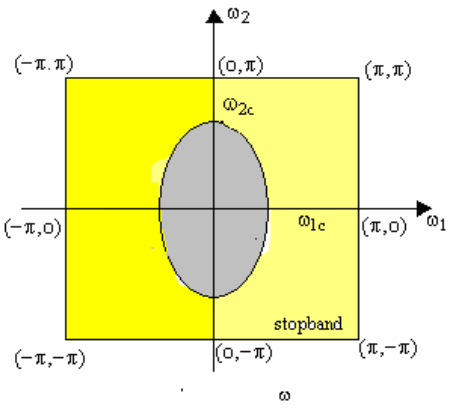

Figure (8): Frequency bands for an elliptically – support low pass filter with two different cutoff frequencies ω_{1c} and ω_{2c}.

while the stopband is described by the region

$$\left\{ \omega_1, \omega_2 : \left[\left[\frac{\omega_1}{\omega_{1c}} \right]^2 + \left[\frac{\omega_2}{\omega_{2c}} \right]^2 \right] > 1 \right\}$$

It is preferred to use elliptical-support filters when two different sampling rates are used on the two spatial axes. It should be noted that filter banks with elliptical split schemes can be designed with a wide variety of pass- and stop-bands, due the allowance of wide range of variations in choosing α_1 and α_2 values. The design of 2-band elliptically-decomposed filter banks is illustrated via the following example:

Example: It is required to design a 2-band elliptically-decomposed filter bank with cutoff frequencies $\omega_{1c} = \pi/5$ rad. and $\omega_{2c} = \pi/2$ rad. The a zero-phase implemention is also required..

Solution:

First, we may specify that we are going to use the 9th order generalized Chebyshev specifications of reference filter(3) (Abdul-Jabbar J. M.,1997) . It should be noted, here, that

$$\omega_c = \omega_{1c} - 2c\left[\tan^{-1}\left(\frac{\alpha_1 \sin\omega_{1c}}{1+\alpha_1 \cos\omega_{1c}} \right) \right]$$

or

$$\omega_c = \omega_{2c} - 2\left[\tan^{-1}\left(\frac{\alpha_2 \sin\omega_{2c}}{1+\alpha_2 \cos\omega_{2c}} \right) \right]$$

Choosing $\alpha_1 = 0.3$, then for $\omega_{1c} = \pi/5$ rad. ,we calculate $\omega_c = 0.3464$ rad.

Thus for $\omega_{2c} = \pi/2$ rad.,we can calculate $\alpha_2 = 0.55$.

The corresponding digital poles are

$$\delta_0 = 0.4887654$$
$$\delta_1 = 0.5162755 \pm i\ 0.3805178$$
$$\delta_2 = 0.5464452 \pm i\ 0.6138920$$
$$\delta_3 = 0.5567534 \pm i\ 0.7336593$$
$$\delta_4 = 0.5670066 \pm i\ 0.7961278$$

The resulting 1-D all-pass functions $a_0(z)$ and $a_1(z)$ given in (16,b,c) . The resulting analysis bank magnitude responses for the low and high frequency channels are shown in Figure (9,a- b).

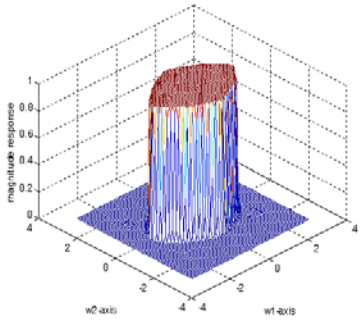

(a) low frequency channel response

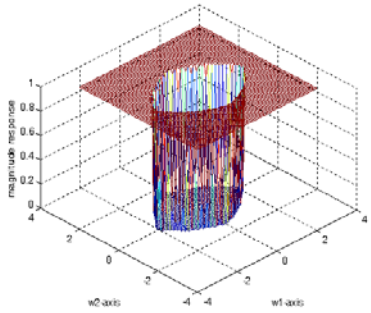

(a) high frequency channel response

Figure (9): 2-band elliptical filter bank response

1) 2-band elliptical directionally-decomposed

If the specification of reference filter-2 (Abdul-Jabbar J. M.,1997) is used, the corresponding 2-D all phase functions(non-separable) $A_i(z_1', z_2')$,$i = 0,1$ are defined by eqation(17).

The directionally-decomposed filter bank transfer functions $CD_i(z_1, z_2)$,$i = 0,1$ can be found as

$$ED_i(z_1, z_2) = h(z_1, z_2)\, A_i(z_1', z_2') \qquad i = 0,1.$$

where $h(z_1, z_2)$ is defined in (27). The resulting 2-band directionally-decomposed filter bank with circular scheme can be implemented as in Figure(3), but with $a_0(z)$ and $a_1(z)$ being replaced by $A_0(z_1', z_2')$ and $A_1(z_1', z_2')$ given in equation (19), respectively. The resulting responses $ED_0(\omega_1, \omega_2)$ and $ED_1(\omega_1, \omega_2)$ are shown in Figure (10).

2) 4-band and 8-band elliptical directionally-decomposed

To design a 4-elliptical directionally-decomposed filter bank, the specifications given in reference filter-3 can also be band, then all-pass functions are $A_i(z'_1, z_2')$ $i = 0,1$, and $B_i(z_1', z_2')$ $i = 0,1$, as given in (18).

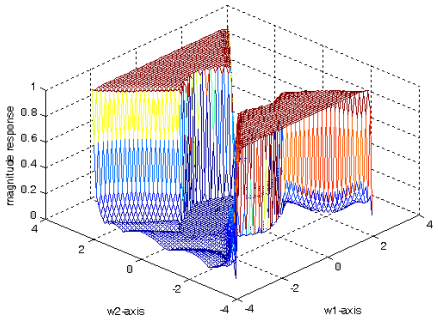

(a)

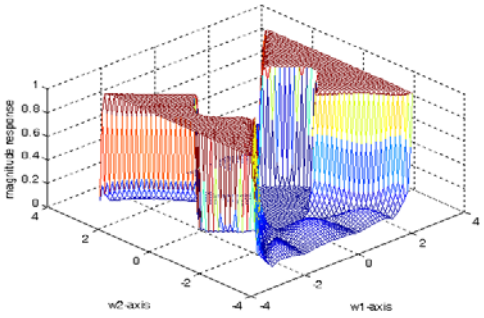

(b)

Figure (10): 2-band elliptical directionally-decomposed filter bank responses.

(a) $ED_0(\omega_1, \omega_2)$ (b) $ED_1(\omega_1, \omega_2)$

The resulting magnitude responses $ED'(\omega_1,\omega_2)$ *for* $i=0,1,2,3$ are shown in Figure (11) and given by

$$ED'_i(z_1,z_2)=h(z_1,z_1)\frac{1}{4}[A_0(z_1,z_2)+A_1(z_1,z_2)][B_0(z_1,z_2)\mp B_1(z_1,z_2)] \quad , \quad for\ i=0,1.$$

and

$$ED'_i(z_1,z_2)=h(z_1,z_1)\frac{1}{4}[A_0(z_1,z_2)-A_1(z_1,z_2)][B_0(z_1,z_2)\mp B_1(z_1,z_2)] \quad , \quad for\ i=2,3.$$

where $h(z_1,z_2)$ is given in (27).

similarly, 8-band elliptical directionally-decomposed filter bank can be designed by using the analysis in section (4). The corresponding 8-band elliptical directionally-decomposed filter bank transfer function can be written as

$$ED''_i(z_1,z_2)=h(z_1,z_2)[\frac{1}{8}[A_0(z_1,z_2)+A_1(z_1,z_2)][B_0(z_1,z_2)+B_1(z_1,z_2)][C_0(z_1,z_2)\mp C_1(z_1,z_2)]]$$

$for\ i=0,1$

$$ED''_i(z_1,z_2)=h(z_1,z_2)[\frac{1}{8}[A_0(z_1,z_2)+A_1(z_1,z_2)][B_0(z_1,z_2)-B_1(z_1,z_2)][C_0(z_1,z_2)\mp C_1(z_1,z_2)]]$$

$for\ i=2,3$

$$ED''_i(z_1,z_2)=h(z_1,z_2)[\frac{1}{8}[A_0(z_1,z_2)-A_1(z_1,z_2)][B_0(z_1,z_2)+B_1(z_1,z_2)][C_0(z_1,z_2)\mp C_1(z_1,z_2)]]$$

$for\ i=4,5$

$$ED''_i(z_1,z_2)=h(z_1,z_2)[\frac{1}{8}[A_0(z_1,z_2)-A_1(z_1,z_2)][B_0(z_1,z_2)-B_1(z_1,z_2)][C_0(z_1,z_2)\mp C_1(z_1,z_2)]]$$

$for\ i=6,7$

where $h(z_1,z_2)$ is given in (27).

The resulting responses $ED''_i(\omega_1,\omega_2)$ *for* $i=0,1,2,3,4,5,6,7$ are shown in Figure (12,a- h), respectively. All the above mentioned split-schemes are to be used for a new proposed contourlet transform(called elliptical contourlet) in the next section.

7. Eilliptical-Support Directional Filter Bank (Eilliptical Contourlet)

Elliptical contourlet can be implemented by elliptical supports and directional filter bank (EDFB) which decomposes images into directional subbands at multiple scales. The EDFB is a cascade of a elliptically-support decomposition and a elliptical directional filter bank as shown in Figure (13a). The EDFB is a elliptically sampled filter bank that decomposes images into any power of two-number of directions. Due to the EDFB `s cascaded structure, the multiscale elliptical and directional decompositions are independent of each other. One can decompose each scale into any arbitrary power of two-number of orientations and different scales can be divided into different numbers of orientations. Figure (13b). shows a typical frequency division of the elliptical contourlet transform where the four scales are divided into two , four, eight subbands from coarse to fine scales, respectively.

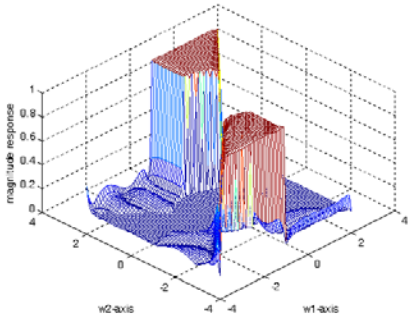

(a)

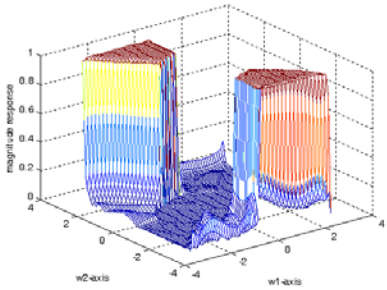

(b)

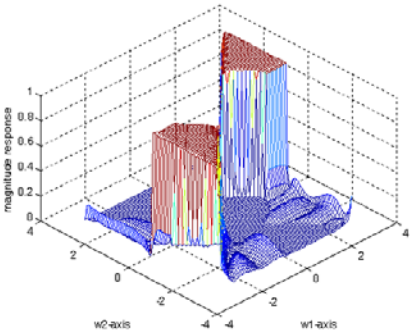

(c)

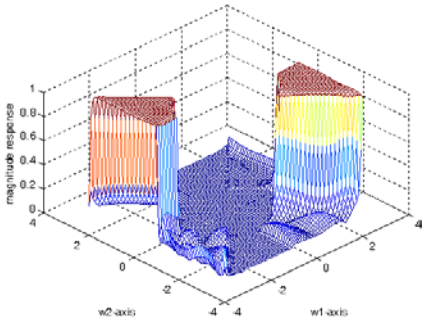

(d)

Figure (11): 4-band circular directionally-decomposed filter bank

responses.

(a) $ED'_0(\omega_1,\omega_2)$ (b) $ED'_1(\omega_1,\omega_2)$

(c) $ED'_2(\omega_1,\omega_2)$ (d) $ED'_3(\omega_1,\omega_2)$

8. Application of EDFB

The EDFB method can be implemented by the following proposed algorithm:

(1) Use reference filter-1, then, the 1-D all-pass functions $a_0(z)$ and $a_1(z)$ can be formed as given in (16(c)) and (16(d)), respectively.
(2) Apply 8-band DFB as given in section(3).
(3) Apply EFB as given in section(4), then, decomposed 8-band EDFB.
(4) Read original image $a(r,c)$, where r is a row and c is a column.
(5) Apply EDFB by the following steps:
   (a) Apply the elliptically-support scheme for the input image $a(r,c)$,outputs are a coarse approximation **c** and a difference **d**.

(b) Applying Fast Fourier Transformation (FFT) to a difference **d** in step (a) above:

$$D(n,m) = FFT(d(r,c)). \qquad (28)$$

(c) Calculate $D(n,m) * ED''_i(\omega_1,\omega_2)$, for $i = 0,1,2,3,4,5,6,7$

where $D(n,m)$ is defined in equation (28), and $ED''_i(\omega_1,\omega_2)$ is EDBF.

(c) Apply FFT^{-1} to the output of step (c).

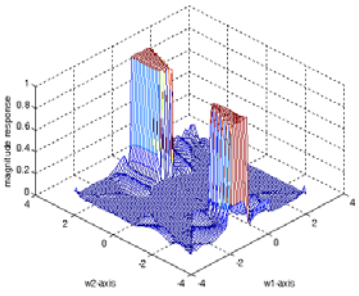

(a)

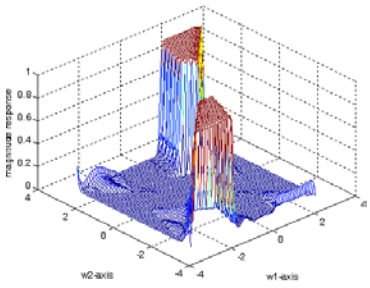

(b)

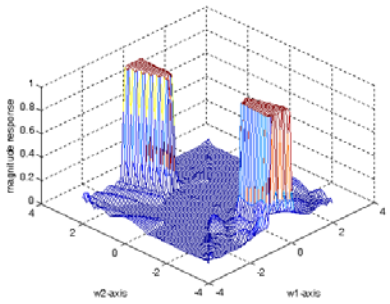

(c)

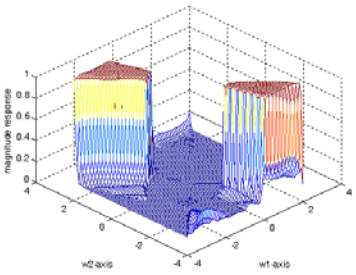

(d)

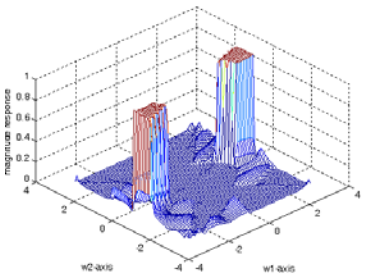

(e)

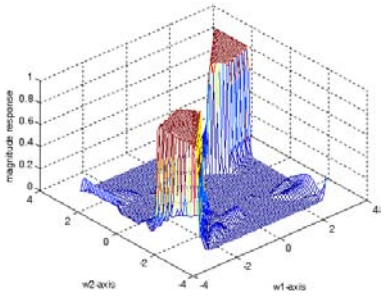

(f)

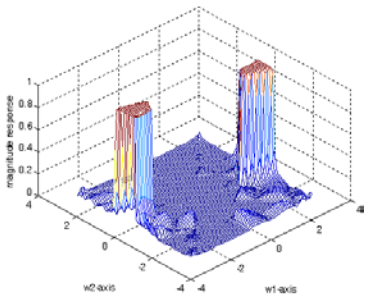

(g)

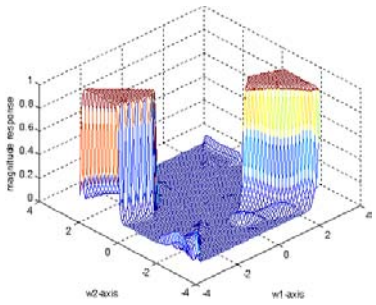

(h)

Figure(12): 8-band elliptical directionally-decomposed filter bank

responses.

(a) $ED_0''(\omega_1,\omega_2)$ (b) $ED_1''(\omega_1,\omega_2)$ (c) $ED_2''(\omega_1,\omega_2)$

(d) $ED_3''(\omega_1,\omega_2)$ (e) $ED_4''(\omega_1,\omega_2)$ (f) $ED_5''(\omega_1,\omega_2)$

(g) $ED_6''(\omega_1,\omega_2)$ (h) $ED_7''(\omega_1,\omega_2)$

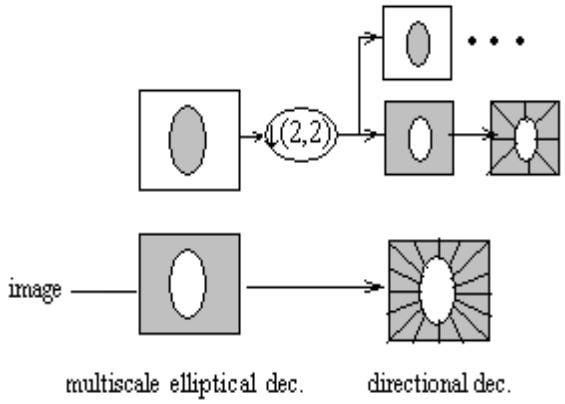

(a)

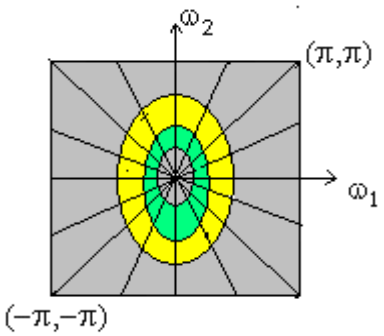

(b)

Figure(13): (a)Elliptically-support directional filter bank structure that implements the discrete elliptical contourlet transform.

(b) A typical elliptical contourlet frequency partition scheme.

9. Objective Measurement

The assessment parameters that are used to evaluate the performance of noise reduction are Noise Variance, Noise Mean Value, Noise Standard Deviation, Deflection Ratio, and Pratt's figure of Merit (Cohen A.,Daubechies I.and Feauveau J.C.,1992,Mastriani M.,2006). One test image(peppers and Lena images)(Figure(14)) are involved in the comparison study between the application of the classical contourlet and the elliptical contourlet.

A. Noise Mean Value (NMV),Noise Variance (NV), and Noise Standard Deviation(NSD).

NV determines the contents of the vector image. A lower variance gives a "cleaner" image as more noise is reduced, although, it does not necessarily depend on intensity. The formulas for the *NMV*, *NV* and *NSD* calculation are

$$NMV = \frac{\sum_{r,c} I(r,c)}{R*C} \quad (29)$$

$$NV = \frac{\sum_{r,c} (I(r,c) - NMV)^2}{R*C} \quad (30)$$

$$NSD = \sqrt{NV} \quad (31)$$

where *R*C* pixels is the size of the vector image *I*. On the other hand, the estimated noise variance is used to determine the amount of smoothing needed for each case for all filters.

B. Deflection Ratio (DR)

A two performance estimator used in this work is the *DR* proposed by Guo et al H.(1994). The formula for the deflection calculation is

$$DR = \frac{1}{R*C} \sum_{r,c} \left(\frac{I(r,c) - NMV}{NSD} \right) \quad (32)$$

C.Pratt's figure of merit (FOM)

To compare the edged preservation performances of different noise reduction schemes, the Pratt's figure of merit is adopted which can be defined as:

$$FOM = 1 - \frac{\alpha}{1 + \beta * DR} \quad (33)$$

where $\alpha = 0.5776$, and $\beta = 2.08 \times 10^{13}$. FOM ranges between 0 and 1, with unity for ideal edge detection.

The assessment parameters *NMV*, *NSD*, *DR* and *FOM* are calculated for the peppers and Lena images after being decomposed by classical contourlet and EDFB. The quantitative results of Table (1-2) show that the numerical result for peppers and Lena test images. From Table (1-2), it can be seen that the elliptical contourlet gives a better value for the objective measures than the ordinary contourlet transform.

Figure(14): Original images of Peppers and Lena of size 256 × 256.

Table(1) Peppers image

	Contourlet Transform.				Elliptical Contourlet Transform.			
band	NMV	NSD	DR	FOM	NMV	NSD	DR	FOM
1	0092.0	0134.0	1904.4e-015	4687.0	0089.0	0133.0	1868.9e-015	5151.0
2	0086.0	0114.0	7194.2e-015	4533.0	0083.0	0112.0	8977.6e-016	4306.0
3	0096.0	0146.0	9521.6e-015	4954.0	0094.0	0146.0	1464.3e-015	4579.0
4	0088.0	0113.0	9676.2e-015	4560.0	0085.0	0112.0	0395.2e-015	4459.0
5	0080.0	0109.0	2.4713e-017	0.4227	0076.0	0.0106	6.9695e-015	4955.0
6	0088.0	0135.0	4858.4e-015	4717.0	0082.0	0134.0	2360.1e-015	4369.0
7	0090.0	0.0146	9556.1e-016	4247.0	0085.0	0144.0	0994.4e-015	4678.0
8	0079.0	0108.0	5404.5e-015	4821.0	0076.0	0105.0	6203.2e-015	4523.0

Table(2) Lena image

	Contourlet Transform.				Elliptical Contourlet Transform.			
band	NMV	NSD	DR	FOM	NMV	NSD	DR	FOM
1	0.0108	0.0123	6.8437e-015	0.4944	0.0104	0.0120	4.4077e-015	0.4709
2	0.0113	0.0156	5.1633e-015	0.4784	0.0108	0.0152	1.0806e-014	0.5284
3	0.0139	0.0162	8.7584e-015	0.5114	0.0133	0.0157	3.6909e-015	0.4636
4	0.0079	0.0105	1.3583e-015	0.4383	0.0078	0.0105	7.0387e-015	0.4962
5	0.0059	0.0070	2.1044e-015	0.4466	0.0059	0.0070	2.8177e-015	0.4544
6	0.0080	0.0107	1.1348e-015	0.4357	0.0067	0.0091	2.9759e-015	0.4561
7	0.0096	0.0120	3.6020e-015	0.4627	0.0087	0.0118	4.5552e-015	0.4724
8	0.0054	0.0059	4.2408e-015	0.4692	0.0033	0.0035	5.0476e-015	0.4773

Conclusion

In this work, we propose a new form elliptical contourlet transform is based on elliptically-support, directionally structures. The idea is based on using a elliptical-split scheme followed by a multiresolution DFB with many levels of decomposition. The proposed elliptical contourlet transform has been discussed and an execution algorithm has been adopted for the calculation of such transform. The resulting detailed peppers and Lena images have been compared to the corresponding detailed images due to the application of the classical contourlet transform. From the objective measures point of view, the resulting assessment parameters(such as, NMV,NV,NSD, DR, and FOM) have indicated the superiority of such a proposal.

References

[1]Abdul-Jabbar J. M.,"**Design procedure of two-dimensional digital filter and filter bank,**"Ph.D. Thesis, Dept.computer, college of Eng. Unv. of Basrah, September 1997.

[2]Bamberger R. H. ,Smith M. J.T.,"**A filter bank for the directional decomposition of images**; **theory and design** ," IEEE Trans. Signal Processing , 40(4), 882-893, April 1992.

[3]Burt P. J., Adelson E. H., " **The Laplacian pyramid as acompact image code",** IEEE Trans.on Communications ,.31(4),532- 540 ,1983.

[4]Cohen A. , Daubechies I., and Feauveau J. C., "**Biorthogonal bases of compactly supported wavelets**," Commn, on Pure and Appl, 485-560, 1992.

[5]Do M. N.,Vetterli M.,"**The contourlet transform: An efficient directional multiresolution image representation**" IEEE Trans. Image Proc.,14(12), 2091-2106, Dec, 2005.

[6] Do M. N.,Vetterli M**.** "**Contourlets**", in:J. Stoeckler, G. V.Welland(Eds.), Beyond Wavelets,pp.1-27.,Academic Press,, 2003.

[7] Do M. N., Vetterli M., "**Frame reconstruction of the Laplacian pyramid** ,"IEEE Int1. Conf. On Acoustics, speech, and signal processing 2001.

[8] Do M. N., Vetterli M, "**Framing pyramids**," IEEE Trans.Signal Proc., 51(9). Sep. 2003.

[9] Mallat S., "**A wavelet tour of signal processing"**, Academic Press, New York, 1998.

[10] Mastriani M. , " **New wavelet-based superrsolution algorithm for speckle reduction in SAR images,"** International Journal of Computer Science ,1(4), 291-298, 2006.

[11] Po D. Y. D., Do M. N., "**Directional multiscale modeling of images using the contourlet transform**,"IEEE Trans.on Image Processing, June 2004.

تحويل الكنتور الناقصي وتطبيقه على تمثيل الصور

بشرى عزيز طه

قسم الرياضيات ، كلية العلوم ، جامعة البصرة،البصرة-العراق.

الخلاصة

يتضمن البحث دراسة أسلوب جديد يعالج حافات الصور، وخاصة المنحنية منها، ويسمى بتحويل الكنتور التناقصي. ثم قارنا هذا التحويل مع الطريقة الكلاسيكية المعروفة بتحويل الكنتور،فأثبت التحويل الجديد جدواه من خلال القياسات الكمية والنوعية.